environmental microbiology

Environmental Microbiology (2022) **24**(4), 2000–2012 doi:10.1111/1462-2920.15971

Energy-conserving dimethyl sulfoxide reduction in the acetogenic bacterium *Moorella thermoacetica*

Florian P. Rosenbaum,[1] Anja Poehlein,[2] Rolf Daniel[2] and Volker Müller[1*]

[1]*Department of Molecular Microbiology & Bioenergetics, Institute of Molecular Biosciences, Johann Wolfgang Goethe University, Frankfurt, Germany.*

[2]*Genomic and Applied Microbiology & Göttingen Genomics Laboratory, Institute of Microbiology and Genetics, Georg-August University Göttingen, Göttingen, 37077, Germany.*

Summary

Moorella thermoacetica **is one of the well-studied thermophilic acetogenic bacteria. It grows by oxidation of organic substrates, CO or H_2 coupled to CO_2 reduction to acetate. Here, we describe that *M. thermoacetica* can also use dimethyl sulfoxide as terminal electron acceptor. Growth of *M. thermoacetica* on glucose or $H_2 + CO_2$ was stimulated by dimethyl sulfoxide (DMSO). Membranes showed a DMSO reductase activity, that was induced by growing cells in presence of DMSO. The enzyme used reduced anthraquinone-2,-6-disulfonate, benzyl- and methyl viologen as electron donor, but not NAD(P)H. Activity was highest at pH 5 and 60°C, the Km for DMSO was 2.4 mM. Potential DMSO reductase subunits were identified by peptide mass fingerprinting; they are encoded in a genomic region that contains three potential *dmsA* genes, three *dmsB* genes and one *dmsC* gene. Transcriptome analysis revealed that two different *dmsAB* gene clusters were induced in the presence of DMSO. The function of these two and their predicted biochemical features are discussed. In addition, the data are in line with the hypothesis that *M. thermoacetica* can use DMSO alongside CO_2 as electron acceptor and DMSO reduction is catalysed by an energy-conserving, membrane-bound electron transport chain with DMSO as final electron acceptor.**

Introduction

The methylated sulfur compound dimethyl sulfoxide (DMSO) plays an environmentally significant role in the biogeochemical cycle of the anti-greenhouse gas dimethyl sulfide (DMS) (Xiong *et al*., 2016). DMS plays a major role in the sulfur cycle, especially the marine environment, that contributes around 80% to the globular DMS flux (Watts, 2000). In marine environments, DMS is produced from dimethylsulfoniopropionate (DMSP) under oxic conditions by algae and phytoplankton and under anoxid conditions by DMSO respiring microorganism (Zinder and Brock, 1978; Curson *et al*., 2011; Kappler and Schäfer, 2014). In the atmosphere, DMS is photooxidized to DMSO and brought back to Earth with precipitation (McCrindle *et al*., 2005). A broad range of facultative aerobic microorganisms such as members of the gut microbiome from higher organism, which consume DMSO-contaminated food and water, as well as soil microorganisms can make use of DMSO as (alternative) electron acceptor for an energy-conserving, anaerobic respiration (Bilous and Weiner, 1985a, b; Lorenzen *et al*., 1994; Xiong *et al*., 2016). The family of DMSO reductases is diverse with more than 25 different types of enzymes including, for example, DMSO reductases and formate dehydrogenases (Magalon *et al*., 2011, Zhang *et al*., 2011, Grimaldi *et al*., 2013). There are two types of DMSO reductases know, the Dor-type (present in *Rhodobacter capsulatus*) and the Dms-type (present in *Escherichia coli*) (Kappler and Schäfer, 2014). A structure for the Dor-type DMSO reductase has been published as well as the predicted function of this type of DMSO reductases (Schindelin *et al*., 1996). The reduction of DMSO is a two-step process; in the first step, DMSO is reduced to DMS thereby oxygen is bound to the molybdenum as oxo ligand. In the second step, two electrons and two protons are required to release the oxygen in form of water and to reduce molybdenum back to the Mo(IV) state, capable to reduce DMSO again (Equation 1) (Schindelin *et al*., 1996).

$$DMSO + 2H^+ + 2e^- \rightarrow DMS + H_2O \quad (1)$$

Received 7 February, 2022; revised 2 March, 2022; accepted 7 March, 2022. *For correspondence. E-mail vmueller@bio.uni-frankfurt.de; Tel. (+49)-69-79829507; Fax (+49)-69-79829306.

DMSO reduction was biochemically and genetically evaluated in greater detail as well in *E. coli*, but a structure for this type of DMSO reductase is still not available (Bilous and Weiner, 1985a, b; Bilous *et al*., 1988; Weiner *et al*., 1988; Sambasivarao and Weiner, 1991, Kappler and Schäfer, 2014). This facultative aerobic, DMSO-respiring enterobacterium has two operons both encoding a DMSO reductase, the phenotypically silent *ynfEFGHI* and the active *dmsABC* operon (Lubitz and Weiner, 2003). Further studies revealed that the *ynfEFGHI* operon encodes for a protein complex involved in the reduction of selenate (Guymer *et al*., 2009; Fujita *et al*., 2021). The functional periplasmic-oriented protein consists of three subunits DmsA, B and C (Lubitz and Weiner, 2003). The membrane anchor DmsC transfers electrons from ubiquinone *via* the iron–sulfur subunit DmsB to the molybdopterin-containing catalytic subunit DmsA (Cammack and Weiner, 1990; Sambasivarao and Weiner, 1991; Weiner *et al*., 1993).

In contrast to the well-studied facultative aerobic microorganisms much less is known about DMSO metabolism in strict anaerobes. In marine environments, some sulfate reducing bacteria have been described to use DMSO instead of sulfate but little is known about the enzymes involved and whether or not DMSO reduction is energy conserving (Zinder and Brock, 1978; Jonkers *et al*., 1996). In terrestrial habitats, CO_2 reducing microbes such as the methanogenic archaea or the acetogenic bacteria predominate (Drake *et al*., 2008; Thauer *et al*., 2008). Methanogens are metabolically rather restricted and can grow by CO_2 reduction, acetate oxidation or methyl-group disproportionation; CO_2 cannot be substituted by any alternative electron acceptor (Thauer *et al*., 2008). In contrast, acetogenic bacteria are metabolically much more versatile (Drake *et al*., 2008; Schuchmann and Müller, 2016). All acetogens have in common that they can reduce CO_2 to acetate via an ancient ATP-neutral pathway – the Wood–Ljungdahl pathway (Müller, 2003; Ragsdale and Pierce, 2008). The electron donor can be either molecular hydrogen, carbon monoxide or an organic substrate (Schuchmann and Müller, 2014). Under autotrophic conditions, ATP is generated by a chemiosmotic mechanism (Müller, 2003; Schuchmann and Müller, 2014).The ion gradient is generated either by the Rnf- or Ech-complex and Na^+ or H^+ can be the coupling ions for both respiratory complexes (Biegel and Müller, 2010; Biegel *et al*., 2011; Schoelmerich and Müller, 2019). The ion gradient is then used to drive ATP synthesis by a Na^+- or H^+-dependent ATP synthase (Heise *et al*., 1992; Das and Ljungdahl, 1997; Rosenbaum and Müller, 2021). Rnf and Ech both use reduced ferredoxin as electron donor and NAD or protons, respectively, as electron acceptor (Biegel and Müller, 2010; Schoelmerich and Müller, 2019). Both NADH and molecular hydrogen are used as reductants in the WLP of CO_2 fixation. Thus, the respiratory complexes are hooked up to the WLP with the aim to reoxidize the electron carriers and to fix CO_2. Thus, the respiratory enzymes could, in principle, be hooked up to other electron consuming pathways. Indeed, some acetogens are known to use alternative electron acceptors instead of CO_2 (Fig. 1). These include aromatic acrylate groups (the acrylate side chain of aromatic compounds), fumarate, or nitrate (Dorn *et al*., 1978; Tschech and Pfennig, 1984; Seifritz *et al*., 1993; Fröstl *et al*., 1996; Misoph *et al*., 1996). Little is known about the biochemistry of fumarate and nitrate reduction in acetogenic bacteria and whether or not these pathways are energy conserving. In contrast, caffeate reduction has been studied in some detail in *Acetobacterium woodii*; the enzymes and genes involved are known and despite the Rnf complex there is no other energy conserving reaction (Imkamp and Müller, 2002; Dilling *et al*., 2007; Imkamp *et al*., 2007; Hess *et al*., 2013). Thus, caffeate serves as electron sink, like CO_2. Astonishingly, sulfur compounds have not been described as alternative electron acceptors in acetogens. However, an abstract from the 1991 annual conference of the American Society for Microbiology noticed growth of the thermophilic acetogen *Moorella thermoacetica* on alcohols in the presence of thiosulfate and DMSO (Beaty and Ljungdahl, 1991). This may imply that *M. thermoacetica* may use DMSO (and thiosulfate) as electron acceptor. To address this question we conducted physiological, biochemical and molecular studies whose results are in accordance with the notion that *M. thermoacetica* can use DMSO as electron acceptor in an energy-conserving electron transport chain.

Results

DMSO stimulates autotrophic and heterotrophic growth of M. thermoacetica

To analyse the effect of DMSO on heterotrophic growth of *M. thermoacetica*, cultures were grown in bicarbonate (CO_2/HCO_3^-)-buffered complex medium with glucose as carbon and energy source supplemented with 20 mM DMSO; cultures were transferred at least three times before the growth experiments were started. Cultures grown in the absence of DMSO had a doubling time of 8.06 h, corresponding to a growth rate μ of 0.08 h^{-1}, and reached a maximal OD_{600} of 0.40 (Fig. 2A). In contrast, the presence of DMSO led to a decreased doubling time of 4.60 h, corresponding to an increased growth rate of 0.15 h^{-1}, and the final optical density also increased to 0.51.

Next, we analysed the effect of DMSO on autotrophic growth on $H_2 + CO_2$. Growth on $H_2 + CO_2$ is rather poor with a doubling time of 69.3 h ($\mu = 0.01$ h^{-1}) and a final OD_{600} of 0.1 (Fig. 2B). Again, addition of DMSO

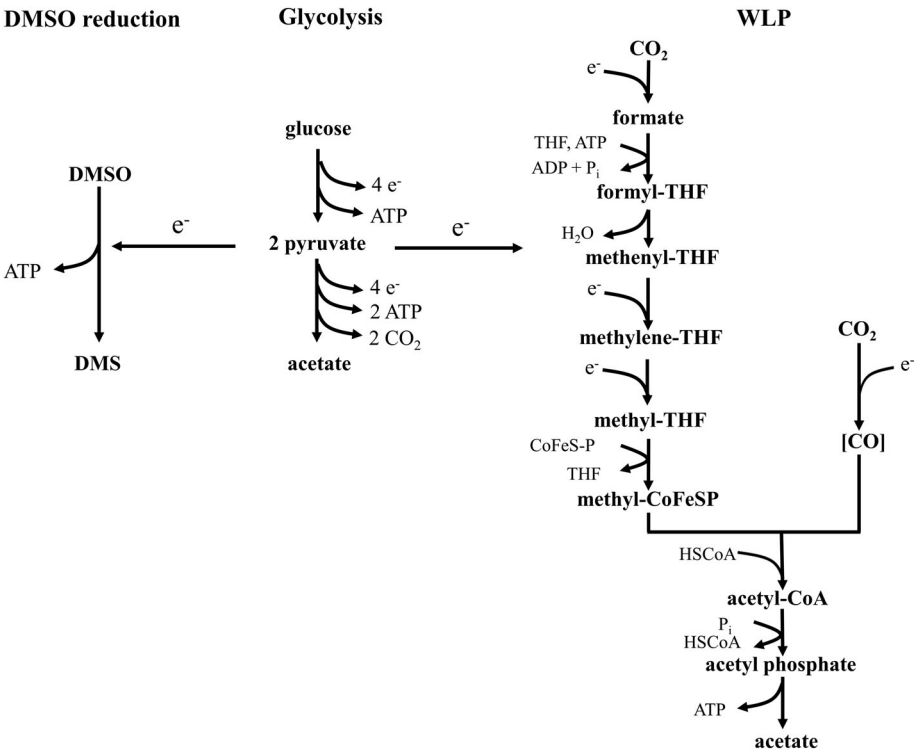

Fig. 1. Model for the oxidation of glucose coupled to reduction of CO_2 or an alternative electron acceptor in acetogenic bacteria. WLP, Wood–Ljungdahl pathway; THF, tetrahydrofolate; CoFeS-P, corrinoid iron–sulfur protein; HSCoA, coenzyme A; [CO], enzyme bound CO.

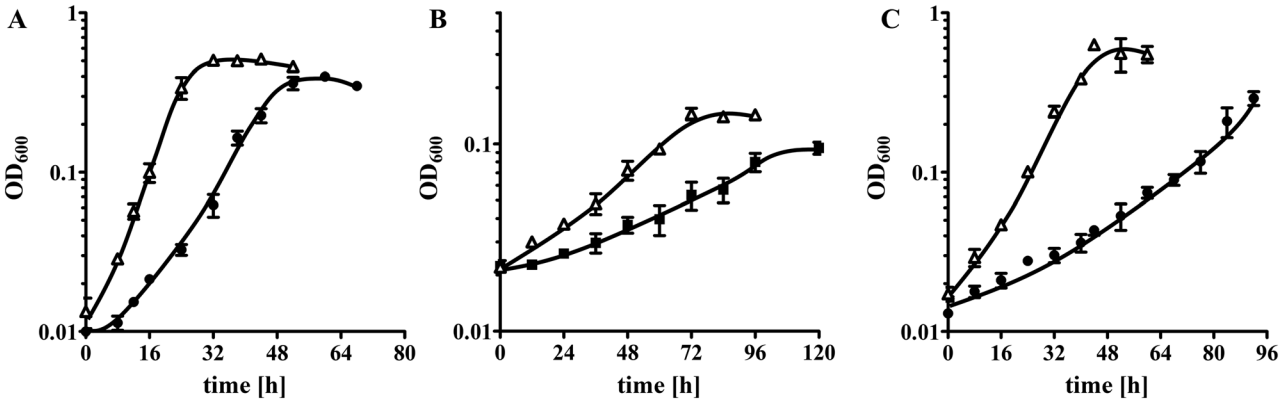

Fig. 2. Growth of *M. thermoacetica* under substrate-limiting conditions in the presence or absence of DMSO. Cells were grown in bicarbonate-buffered medium under either a $N_2 + CO_2$ (80:20 [v/v]) atmosphere (A) or $H_2 + CO_2$ (80:20 [v/v]) (B). In (C) cultures were grown in phosphate-buffered medium under a 100% N_2 atmosphere. Cells were grown either heterotrophically using 5 mM glucose (A and C) or autotrophically using 2×10^5 Pa $H_2 + CO_2$ (B) with DMSO supplementation (Δ) or without (●) ($n = 3$, SD). All cultures were grown at 55°C and the optical density was monitored at 600 nm.

stimulated growth: the doubling time decreased to 23.1 h ($\mu = 0.03\ h^{-1}$) and the final OD to 0.15.

To test whether DMSO can substitute for CO_2 as electron acceptor, growth experiments were performed using 100% N_2 instead of $N_2 + CO_2$ (80:20 [v/v]) and phosphate – rather than bicarbonate-buffered complex medium. Cultures grown with 5 mM glucose and in the absence of any electron acceptor grew poorly with a doubling time of 34.6 h ($\mu = 0.02\ h^{-1}$) to a final optical density of 0.29 (Fig. 2C). The addition of DMSO reduced the doubling time by 75% to 8.62 h ($\mu = 0.08\ h^{-1}$) and the final OD increased by 217% to 0.63. These experiments are in line with the hypothesis that DMSO serves as (additional) electron acceptor.

Metabolic profile of M. thermoacetica *growing on glucose in the presence of DMSO*

To address the question whether or not *M. thermoacetica* can reduce DMSO and whether the metabolites formed changed in the presence of DMSO, growth experiments were performed. In the absence of DMSO, *M. thermoacetica*

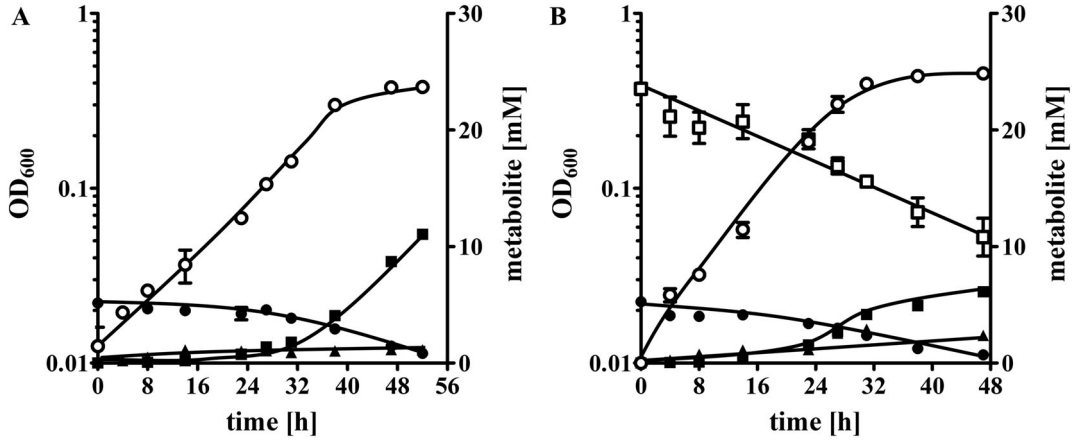

Fig. 3. DMSO shifts the metabolite profile during glucose fermentation. Cells were grown in bicarbonate-buffered medium under a N_2 + CO_2 (80:20 [v/v]) atmosphere at 55°C with 5 mM glucose in the absence (A) or presence (B) of 20 mM DMSO. OD_{600} (○), glucose (●), acetate (■), lactate (▲) and DMSO (□) concentrations were monitored by HPLC ($n = 2$; SD).

oxidized 5.2 ± 0.38 mM glucose to 11.0 ± 0.37 mM acetate as main product. Additionally, small amounts of approximately 1 mM of lactate were detected as well (Fig. 3A). In the presence of DMSO a shift in the metabolic profile as well as an increase of the OD_{600} was observed. Within 47 h *M. thermoacetica* reached an OD_{600} of 0.45, which is an increase of 19.5% compared to cultures growing in the absence of DMSO. The 4.6 mM glucose was oxidized and in addition 13.9 mM DMSO were reduced. Cultures grown in the presence of DMSO produced 6.1 ± 0.23 mM acetate, which is 45% less compared to cultures lacking DMSO (Fig. 3B). DMSO had apparently no effect on lactate production.

Resting cell experiments

To analyse the fermentation balance, first cells were grown on glucose and resting cells were prepared. Resting cells started immediately to consume glucose at a rate of 1.99 ± 0.04 mM h^{-1} and produced acetate at a rate of 4.96 ± 0.21 mM h^{-1}. Again, traces of lactate (2.76 ± 0.02 mM) were formed (Fig. 4A). The ratio of glucose consumed and acetate and lactate produced was 1:2.6:0.29. Resting cells pregrown on glucose + DMSO consumed glucose at a rate of 3.40 ± 0.43 mM h^{-1} and reduced DMSO at a rate of 6.28 ± 0.12 mM h^{-1}. As in growing cells, lactate production was not affected by the presence of DMSO. The metabolites acetate and lactate were produced at a rate of 6.24 ± 0.12 mM h^{-1} and 1.02 ± 0.07 mM h^{-1}, respectively (Fig. 4B). The ratio of glucose consumed, acetate and lactate produced and DMSO reduced was 1:2.0:0.34:1.50, indicating that approximately 41% of the electrons obtained from glucose metabolism were used to reduce DMSO. As seen with growing cells, DMSO was reduced and less acetate was produced. DMSO was also reduced with H_2 as electron donor (data not shown).

Identification and characterization of the membrane-bound DMSO reductase activity

If DMSO serves as electron acceptor, it should be reduced by cell-free extracts of *M. thermoactica*. To test this, cells were grown in carbonate-buffered medium with glucose as carbon and energy source and the presence or absence of DMSO. Cells were harvested by centrifugation, cell-free extracts were prepared and DMSO-dependent oxidation of the reduced artificial electron carrier benzyl viologen (BV) was monitored. First, we measured the specific activity of the DMSO reductase in cell-free extract and continued to separate the cell-free extract into membranes and cytoplasm. The specific activities amounted to 0.36 and 0.03 U mg^{-1} for the membrane fraction and the cytoplasmic fraction, respectively (Fig. 5A), further calculations reveals that 87% of the activity was found in the membrane fraction (2.60 ± 0.17 U) whereas only 13% was present in the cytoplasm (0.71 ± 0.03 U) (Fig. 5B). Additionally, the highest activity was measured in membranes prepared from mid-exponential cells with a specific activity of 0.38 ± 0.02 U mg^{-1} compared to 0.18 ± 0.03 U mg^{-1} and 0.20 ± 0.04 U mg^{-1} in early- or late-exponential cells (Fig. 5C). Cells grown in the absence of DMSO had a negligible DMSO-dependent BV oxidation rate, but this rate increased by 1556% to 0.36 U mg^{-1} in DMSO-grown cells, indicating a strong induction of DMSO reduction by DMSO (Fig. 5D). As expected, not only benzyl viologen but also methyl viologen (MV) served as electron donor (0.43 ± 0.01 U mg^{-1}). Interestingly, also the reduced soluble quinone analogue anthraquinone-2,6-disulfonate (AQDS) was oxidized in a DMSO-dependent manner by membranes with a specific activity of 0.15 ± 0.01 U mg^{-1} (Fig. 5E). BV-dependent DMSO reduction by membranes was highest at

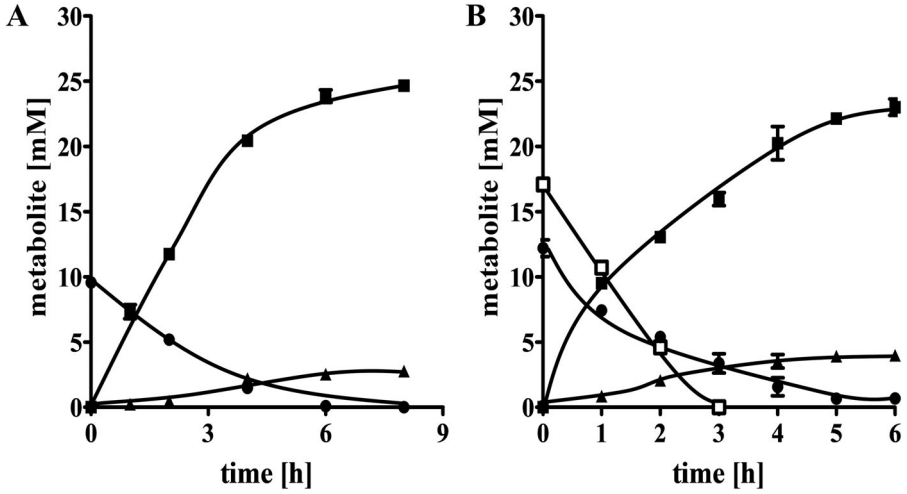

Fig. 4. Glucose-dependent DMSO reduction in resting cells of *M. thermoacetica*. Cells were grown on glucose in the presence or absence of DMSO, harvested in the exponential growth phase and resting cells were prepared. Cell suspensions were supplemented with 10 mM glucose (A) or 10 mM glucose + 20 mM DMSO (B). The assays were performed in 120 ml serum bottles filled with bicarbonate-containing resting cell buffer under a $N_2 + CO_2$ (80:20 [v/v]) gas atmosphere at ambient pressure. The final assay volume was 20 ml and the assays were preincubated at 55 °C for 15 min before the reaction was started by the addition of glucose. Glucose (●), acetate (■), lactate (▲) and DMSO (□) concentrations were monitored by HPLC ($n = 3$; SD).

60 °C (0.41 ± 0.03 U mg^{-1}) (Fig. 5F) and at pH 5 (0.48 ± 0.07 U mg^{-1}) (Fig. 5G). At optimal pH and temperature, the specific activity was 0.82 ± 0.05 U mg^{-1}. Furthermore, the Km was determined to be 2.4 mM, which is rather high compared to the Km of 0.18 mM of the purified enzyme of *E. coli* (Fig. 5H) (Simala-Grant and Weiner, 1996).

Identification of proteins potentially involved in DMSO reduction

The genome of *M. thermoacetica* has a gene cluster that encodes proteins similar to the previously mentioned DmsABC DMSO reductase of *E. coli* (Fig. 6, see below). To identify proteins involved in DMSO reduction cells were grown in bicarbonate-buffered medium with glucose as carbon and energy source in the absence or presence of 20 mM DMSO, cells were harvested in the mid-exponential growth phase and membranes were prepared as described above. Membrane proteins were solubilized by Triton X-100 and the solubilized proteins were identified by peptide mass fingerprinting. Among others, the proteins encoded by Mothe_c13700–13710 and by Mothe_c13730–13740 were slightly more abundant (by factor of 2) in cells grown in the presence of DMSO compared to cells grown in the absence of DMSO (data not shown.).

Genetic organization of potential DMSO reductase genes and properties of the deduced proteins

Mothe_c13690–13740 are part of a larger gene cluster that could encode three different DMSO reductases (Fig. 6.). Within this cluster one DmsC-, three DmsB- and three DmsA-subunits are encoded. The membrane anchor DmsC has eight transmembrane helices and is encoded by the 852 bp long gene Mothe_c13690. The corresponding protein has a size of 21.4 kDa and shows an identity of 25% to DmsC of *E. coli* (Table 1.). The 549 bp long gene Mothe_c13660 codes for a 20.5 kDa protein with similarity to DmsB, it harbours two 4Fe-4S cluster and is called hereafter DmsB1. The DmsB subunit is known to transfer electrons from the membrane anchor subunit DmsC to the catalytic subunit DmsA (Xiong *et al*., 2016). Within the cluster two more *dmsB* genes (*dmsB2*; Mothe_c13700 and *dmsB3*; Mothe_c13730) are present; they encode proteins with sizes of 21.4 and 20.1 kDa, respectively. DmsB2 and B3 are predicted to harbour three 4Fe-4S cluster. DmsB1 shares an identity of 41% to DmsB2 and B3, whereas DmsB2 is 62% identical to DmsB3. The putative *dms* cluster codes for three potential DmsA subunits. Mothe_c13670 (DmsA1) encodes for a 74.5 kDa and Mothe_c13710 and 13740 for 88.7 and 95.3 kDa proteins (DmsA2 and A3), respectively. The DmsA proteins differ in size, DmsA1 is the shortest protein with 678 amino acids, whereas A2 and A3 have 799 and 857 amino acids, respectively (Fig. 7.). DmsA2 and A3 have a predicted twin-arginine-motif, indicating that both subunits are periplasmic, whereas A1 lacks this motif. All putative DmsA subunits have a molybdopterin binding domain and one putative 4Fe-4S cluster binding domain (Fig. 7.). The DmsA subunits show a rather low identity to each other, A1 has an identity of 29% and 24% to DmsA2 and A3, whereas A2 and A3 are 37% identical. Furthermore, the DMSO reductase subunits A1-3 and B1-3 were compared to the well characterized DMSO reductase

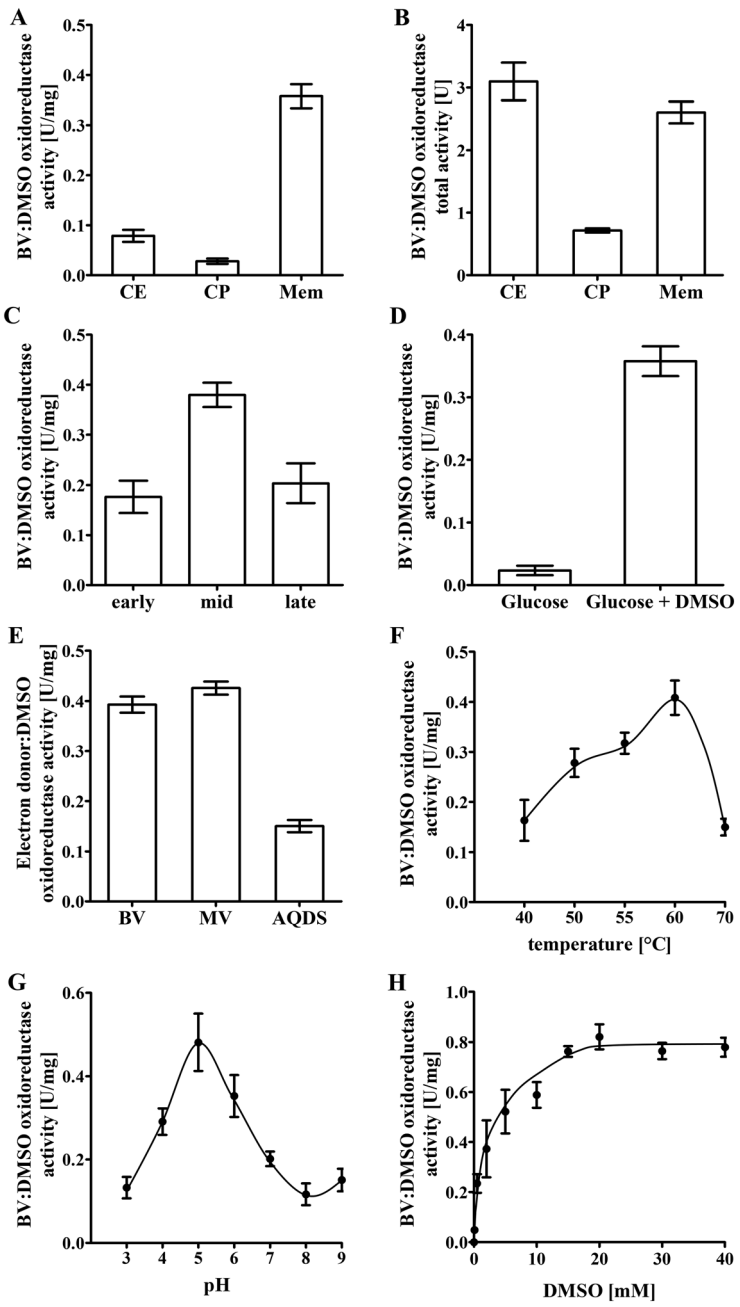

Fig. 5. Biochemical characterization of DMSO reductase. 50–55 μg cell-free extracts, cytoplasm (CE, CP; A and B) or membranes (Mem; all) prepared from cells grown on glucose with DMSO (A–H) and without DMSO (D). CE, CP and Membranes were prepared from mid-exponential (mid) grown cells (A–H). Additionally, Membranes from early- (early) and late-exponential (late) grown cells were used as well (C). Enzyme activity assays were conducted in enzyme buffer 1 (all, except G and H), enzyme buffer 2 (G) or enzyme buffer 3 (H). The electron donors BV (A-H), MV or AQDS (E) were reduced by sodium dithionite, the reaction was started by addition of 20 mM DMSO. 1 mM BV, MV or 0.25 mM AQDS in the reduced state were used as electron donors and their oxidation was measured at 604 or 408 nm, respectively ($n = 3$; SD).

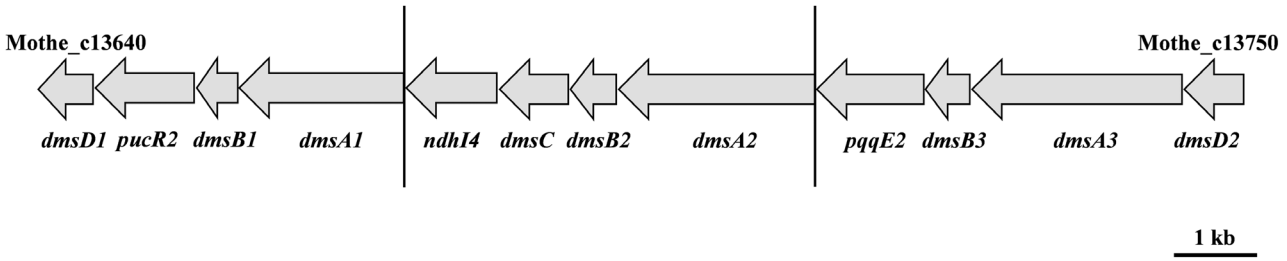

Fig. 6. Genomic organization of the potential DMSO reductases in *M. thermoacetica*. *dmsD1/2*, chaperone; *pucR2*, putative regulator protein; *dmsB1/2/3*, DmsB subunit; *dmsA1/2/3*, DmsA subunit; *ndhI4*, 4Fe-4S ferredoxin, iron–sulfur binding protein; *dmsC*, DmsC subunit; *pqqE2*, radical SAM protein PQQE2.

Table 1. Sequence identity of the putative Dms proteins of *M. thermoacetica* to the corresponding proteins from *E. coli*.

Locus Tag (Mothe_c)	Annotation	mass (kDa)	Identity (%)
13640	Tat proofreading chaperone DmsD	26.0	37[a]
13650	purine catabolism regulatory protein	46.5	-
13660	DmsB1	20.5	43[b]
13670	DmsA1	74.5	27[c]
13680	4Fe-4S ferredoxin, iron–sulfur binding protein	40.4	-
13690	DmsC	30.5	25[d]
13700	DmsB2	21.4	52[b]
13710	DmsA2	88.7	55[c]
13720	Radical SAM protein	51.1	-
13730	DmsB3	20.1	47[b]
13740	DmsA3	95.3	33[c]
13750	Tat proofreading chaperone DmsD	27.5	31[a]

[a]*E. coli* locus tag: b1591.
[b]*E. coli* locus tag: b0895.
[c]*E. coli* locus tag: b0896.
[d]*E. coli* locus tag: b0894.

subunits DmsAB of *E. coli*. DmsA2/B2 shows the highest similarity with 53% and 52%, respectively. DmsA1/A3 and DmsB1/B3 are less similar with identities of around 27%–33% for DmsA1/A3 and 43%–47% for DmsB1/B3, respectively (Fig. 7.). The putative *dms* cluster is surrounded by the genes Mothe_c13640 (681 bp) and 13740 (711 bp) (Fig. 6.). Both genes code for chaperones of 26.0 and 27.5 kDa, which are of 37% and 31% identical to DmsD of *E. coli*, which is known to be involved into the biogenesis of DmsA. Interestingly, the cluster also encodes for one putative SAM-radical protein (PQQE2, Mothe_c13720, 1326 bp, 51.1 kDa), a 4Fe-4S ferredoxin, iron–sulfur binding protein (Ndh4, Mothe_13680, 1152 bp, 40.4 kDa) and a putative regulator (PucR2, Mothe_13650, 403 bp, 46.5 kDa).

Transcriptomic changes during DMSO reduction

To identify gene products involved in DMSO reduction, we compared the transcriptome of cells grown on glucose with DMSO to cells grown in the absence of DMSO in their respective mid-exponential growth phase. Using a log2fold change (FC) of $+2/-2$ and a *P*-adjust value of <0.05 as threshold, a total of 97 genes of all 2594 were differentially expressed (Supplementary Table S1).

The putative DMSO reductase gene *dms*C (FC: $+2.6$) as well as the *dms*B2/A2 (FC: $+2.4$ to $+2.7$) and *dms*B3/A3 (FC: $+3.3$ to $+3.5$) were upregulated in presence of DMSO. The FC of *dms*B1/A1 was below the threshold of ± 2. This corroborates the absence of DsmA1/B1 in the membrane fraction. DmsD (Mothe_c13750; FC: $+3.4$) as well as the gene encoding for a radical SAM protein (Mothe_c13720; FC: $+3.6$) were upregulated in the presence of DMSO.

Since DMSO and CO_2/bicarbonate were apparently used simultaneously, the question arose whether expression of the WLP genes were affected by the presence of DMSO. The expression levels of almost all genes of the WLP were not affected by the presence of DMSO, only

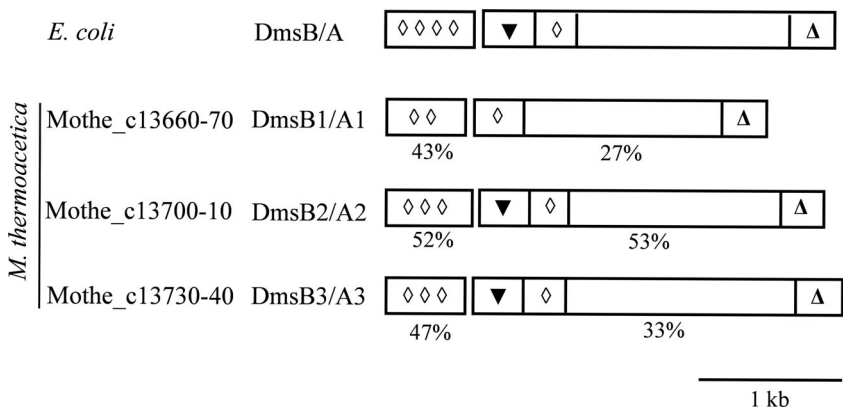

Fig. 7. Comparison of the DMSO reductase subunits DmsA and DmsB. The DMSO reductase subunits DmsA and DmsB of *M. thermoacetica* were compared to the DMSO reductase of *E. coli*. Molybdopterin binding domain (Δ), TAT (twin-arginine translocation) domain (▼), 4Fe-4S binding domain (◊).

the gene encoding for the formyl-THF synthetase (Mothe_c01150) was downregulated 2fold.

Transcript levels of most genes encoding for proteins related to redox balancing such as the *ech1* (Mothe_c09340–09440) and *ech2* genes (Mothe_c22350–22520), both putatively encoding a membrane-bound, ion-translocating Fd:H^+ oxidoreductase, cytochrome biosynthesis (Mothe_c16040, 21490–21500 and 22590–22600), electron-bifurcating NADH-dependent Fd^{2-}:$NADP^+$ oxidoreductase (Nfn/transhydrogenase; Mothe_c15090–15100) and the $NADP^+$-reducing hydrogenase (Mothe_c19180–19230) were also not affected by the presence of DMSO. Genes encoding for the electron-bifurcating hydrogenase (Mothe_c17260–17280; FC: −7.3 to −8.2), the quinone biosynthesis machinery (Mothe_c18740–18780; FC: −2.5 to −3.2) were downregulated. Interestingly, genes encoding for a membrane-bound molybdopterin oxidoreductase (Mothe_c19440–19460; FC: -5.5 to −7.3), were downregulated in the presence of DMSO (Table 2).

Discussion

M. thermoacetica has been the model organism to identify and unravel the pathway of CO_2 fixation in acetogens (Fontaine *et al*., 1942; Ljungdahl, 1986; Wood *et al*., 1986), but astonishingly little is still known about the bioenergetics of CO_2 reduction and the possible use of electron acceptors other than CO_2, only nitrate has been studied in greater detail (Seifritz *et al*., 1993; Fröstl *et al*., 1996; Arendsen *et al*., 1999). Although it has been reported in an abstract of a conference contribution that *M. thermoacetica* may reduce DMSO, data had not been presented (Beaty and Ljungdahl, 1991). Here, we clearly demonstrate that growing as well as resting cells of *M. thermoacetica* are able to reduce DMSO. Although *M. thermoacetica* is able to utilize the methyl group of several methylated compounds as carbon and energy source (Daniel *et al*., 1991; Drake and Daniel, 2004), it could not grow on DMSO as sole carbon and energy source and resting cells pregrown on glucose + DMSO were not able to demethylate DMS (data not shown). The genome of *M. thermoacetica* harbours genes (*dmsAB*) encoding three potential DMSO reductases (Pierce *et al*., 2008). DmsA2B2- and DmsA3B3 are most likely periplasmic, membrane bound enzyme complexes. Both gene clusters encode an additional protein (Ndh4 and PqqE2) whose function is unknown. PqqE encoded in cluster 3 is an iron–sulfur containing oxidoreductase that mediates the first step in PQQ biosynthesis, the radical-mediated formation of a new carbon–carbon bond (Puehringer *et al*., 2008); however, whether the oxidoreductase PQQE2 is involved in electron transfer from the physiological electron donor to the DmsABC complex or it merely serves in assembly/biosynthesis needs to be addressed experimentally. Notably is that only the A2B2 cluster encodes for the entry part of electrons into a possible membrane bound electron transport system, DmsC. The A1B1 cluster also contains a gene encoding an assembly factor and a putative regulator. The A1B1 complex is regulated differently from cluster 2 and 3 as apparent from the peptide mass fingerprint and transcriptome analyses that shows, that the genes were not expressed, and the

Table 2. Expression of genes in response to DMSO.

Locus Tag (Mothe_c)	Annotation	*P*adj	FC
13690	DmsC	4.37×10^{-36}	+2.6
13700	DmsB2	8.03×10^{-18}	+2.4
13710	DmsA2	3.92×10^{-72}	+2.7
13720	Radical SAM protein	4.26×10^{-92}	+3.6
13730	DmsB3	3.25×10^{-43}	+3.5
13740	DmsA3	7.17×10^{-105}	+3.3
13750	Tat proofreading chaperone DmsD	2.22×10^{-48}	+3.4
01150	formate--tetrahydrofolate ligase	4.84×10^{-39}	−2.0
17260	NADP-reducing hydrogenase subunit HndC	8.65×10^{-158}	−7.3
17270	NADP-reducing hydrogenase subunit HndC	7.76×10^{-128}	−7.4
17280	NADP-reducing hydrogenase subunit HndA	6.60×10^{-32}	−8.2
18740	cyclic dehypoxanthine futalosine synthase	5.57×10^{-75}	−3.1
18750	chorismate dehydratase	1.26×10^{-78}	−3.0
18760	aminodeoxyfutalosine synthase	8.55×10^{-80}	−3.0
18770	S-methyl-5′-thioadenosine phosphorylase	5.26×10^{-57}	−2.5
18780	fatty acid metabolism regulator protein	9.29×10^{-50}	−3.2
19440	putative hydrogenase 2 b cytochrome subunit	4.03×10^{-90}	−5.5
19450	tetrathionate reductase subunit B precursor	1.90×10^{-47}	−5.9
19460	perchlorate reductase subunit alpha precursor	1.18×10^{-147}	−7.3

Numbers indicate log2fold change (FC) and the *P*-adjust value (Padj) from glucose + DMSO-grown cells compared to glucose-grown cells without DMSO in the exponential growth phase.

proteins were not found. The A2B2 and A3B3 genes were upregulated during growth in the presence of DMSO and the proteins were found in DMSO-grown cells.

Apparently, DMSO and CO_2 were reduced simultaneously, as evident from the growth curves, the metabolic profile and the transcriptome analyses. Simultaneous use of CO_2 and an alternative electron acceptor is not common in acetogens, but certainly is of big advantage for biotechnological applications. Production of valuable compounds from $H_2 + CO_2$ in natural or engineered strains of acetogens is strongly limited by the negative ATP yield of acetyl-CoA-formation from $H_2 + CO_2$ (Bertsch and Müller, 2015; Katsyv and Müller, 2020). Acetate production (coupled to ATP synthesis) brings the process to a balanced ATP yield, DMSO reduction could do the same. However, this is only possible, if DMSO reduction is energy-conserving, i.e., ATP producing. As mentioned earlier, DMSO respiration is known in *E. coli* and the presence of a DmsABC-complex is in accordance with the hypothesis that DMSO reduction is energy conserving in *M. thermoacetica*. This is corroborated by the observed increase in cell yield and the presence of a membrane anchor known to interact with quinones. Furthermore, this hypothesis is corroborated with the presence of a membrane bound DMSO reductase that can use AQDS as electron acceptor. Future work has to shed light into the biochemistry and bioenergetics of this novel respiratory chain in the model acetogen *M. thermoacetica*.

Materials and methods

Growth conditions

Moorella thermoacetica (DSM 521) was cultivated under anaerobic conditions at 55 °C in bicarbonate-buffered complex medium under an $N_2 + CO_2$ (80:20 [v/v]), $H_2 + CO_2$ (80:20 [v/v]) atmosphere or in phosphate-buffered complex medium under a 100% N_2 atmosphere. The media were prepared according to Sakimoto *et al*. (2016) using the anaerobic techniques described previously (Hungate, 1969; Bryant, 1972). Growth experiments were performed in 120 ml serum bottles (Glasgerätebau Ochs, Bovenden/Lenglern, Germany) filled with 50 ml complex medium, supplemented with 5 or 50 mM glucose with and without 20 mM DMSO. Growth experiments using $H_2 + CO_2$ with and without DMSO were performed with a final pressure of 2×10^5 Pa.

Resting cell experiments

Cells were grown in bicarbonate-containing complex medium in 1 l flasks (Schott AG, Mainz, Germany) filled with 500 ml medium. Cultures were harvested under anoxic conditions at an OD_{600} of 0.4 by centrifugation (Avanti™J-25 and JA-10 Fixed-Angle Rotor; Beckman Coulter, Brea, CA, USA) at 8.000 *g* for 7 min at 4°C and subsequently washed twice with anoxic resting cell buffer (50 mM MOPS, 50 mM $KHCO_3$, 20 mM NaCl, 20 mM $MgSO_4 \times 7\ H_2O$, 20 mM KCl, 2 mM DTE, 4 μM resazurin; pH 7) using the same centrifugation conditions as before. After the second washing step, cells were resuspended in 2 ml buffer, and subsequently, the protein concentration was determined according to Schmidt *et al*. (1963). Resting cell experiments were performed in 120 ml serum bottles using 20 ml resting cell buffer supplemented with cells to a final concentration of 1 mg ml^{-1}. The gas phase was replaced by flushing the flask with $N_2 + CO_2$ (80:20% [v/v]), 20 mM DMSO were added, and after a 15 min preincubation at 55 °C, the reaction was started by adding 5 or 10 mM glucose. The assays were incubated at 55°C and 100 rpm.

Analytical methods

Metabolite analyses were carried out using high-pressure liquid chromatography as described previously (Schwarz *et al*., 2020).

Preparation of cell-free extract and subcellular fraction

M. thermoacetica was cultivated as described above and all steps were carried out in an anaerobic chamber (Coy Laboratories, Grass Lake, USA) containing an $N_2 + H_2$ (95:5 [v/v]) atmosphere. Cultures were harvested at mid-exponential growth phase (OD_{600} of 0.4) by centrifugation (6300 *g*, 7 min, 4°C) and washed twice with anoxic harvest buffer (50 mM Tris–HCl (pH 7.5), 20 mM $MgSO_4 \times 7\ H_2O$, 20% glycerol, 4 mM DTE, 4 μM resazurin). Furthermore, cell-free extracts were also prepared by harvesting cells.

Cell-free extract, cytoplasm and membranes were prepared as described by Rosenbaum *et al*. (2021). To ensure a less harsh cell disruption 50 MPa instead of 120 MPa were used in the French press. For LC/MS–MS analysis, washed membranes were solubilized by adding 1% Triton X-100 and shaking overnight. The protein concentration was measured as described previously (Bradford, 1976).

Enzyme activity assays

All enzyme assays were carried out at 55°C in 1.8 ml anoxic cuvettes (Glasgerätebau Ochs, Bovenden/Lenglern, Germany) filled with enzyme buffer 1 (200 mM KP_i [$K_2HPO_4 + KH_2PO_4$ (pH 8)], 10 mM NaCl) at a final liquid volume of 1 ml in a 100% N_2 gas atmosphere. The pH dependence was measured in buffer 2 (25 mM Tris, 25 mM CHES, 25 mM MES, 25 mM MOPS, 25 mM

citrate (pH 3–9), 10 mM NaCl). The Km was determined using buffer 3 (200 mM K_2HPO_4, 50 mM citrate (pH 5), 10 mM NaCl). DMSO reductase activity was measured with 1 mM BV or MV at 604 nm (εBV/MV = 13.8 mM^{-1} cm^{-1}) or 0.25 mM AQDS at 408 nm (εAQDS = 7.2 mM^{-1} cm^{-1}), which was reduced by sodium dithionite to serve as electron donor. The oxidation BV, MV or AQDS was started by adding 20 mM DMSO.

LC/MS–MS analysis

Solubilized membranes of glucose- and glucose + DMSO-grown cells were analysed by MALDI-TOF analysis, which was performed by the 'Functional Genomics Center Zürich' at the ETH Zürich, Switzerland. The results were analysed using the Scaffold-Proteome Software version 4.10.0 (Proteome Software, Portland, OR, USA).

Transcriptome analysis

The transcriptome of glucose + DMSO-grown cells was compared to the transcriptome of glucose-grown cells. Glucose + DMSO- or glucose-grown cells were cultivated in biological triplicates as described and harvested in the exponential growth phase (OD_{600} 0.4 for both conditions) (Göbbels *et al*., 2021). Harvested cells were resuspended in 800 µl RLT buffer (RNeasy Mini Kit, Qiagen) with β-mercaptoethanol (10 µl ml^{-1}) and cell lysis was performed using a laboratory ball mill. Subsequently 400 µl RLT buffer (RNeasy Mini Kit Qiagen) with β-mercaptoethanol (10 µl ml^{-1}) and 1200 µl 96% [v/v] ethanol were added. For RNA isolation, the RNeasy Mini Kit (Qiagen) was used as recommended by the manufacturer, but instead of RW1 buffer RWT buffer (Qiagen) was also used in order to isolate RNAs smaller than 200 nt. To determine the RNA integrity number (RIN), the isolated RNA was run on an Agilent Bioanalyzer 2100 using an Agilent RNA 6000 Nano Kit as recommended by the manufacturer (Agilent Technologies, Waldbronn, Germany). Remaining genomic DNA was removed by digesting with TURBO DNase (Invitrogen, ThermoFischer Scientific, Paisley, United Kingdom). The Illumina Ribo-Zero plus rRNA Depletion Kit (Illumina, San Diego, CA, USA) was used to reduce the amount of rRNA-derived sequences. For sequencing, the strand-specific cDNA libraries were constructed with a NEBNext Ultra II directional RNA library preparation kit for Illumina (New England BioLabs, Frankfurt am Main, Germany). To assess quality and size of the library samples were run on an Agilent Bioanalyzer 2100 using an Agilent High Sensitivity DNA Kit as recommended by the manufacturer (Agilent Technologies, Waldbronn, Germany). Concentration of the libraries was determined using the Qubit® dsDNA HS Assay Kit as recommended by the manufacturer (Life Technologies GmbH, Darmstadt, Germany). Sequencing was performed on the NovaSeq 6000 instrument (Illumina) using NovaSeq 6000 SP Reagent Kit (100 cycles) and the NovaSeq XP 2-Lane v1.5 for sequencing in the paired-end mode and running 2× 50 cycles. After processing of the 50 bp single-end raw reads with trimmomatic (version 0.39) (Bolger *et al*., 2014), Salmon (v 1.5.2) (Patro *et al*. 2017) was used for mapping of the trimmed paired-end read against the genome of *M. thermoacetica* DSM521 (Poehlein *et al*. 2015). A file containing all annotated transcripts (without rRNA genes) and the whole genome as decoy was prepared with a k-mer size of 11 as mapping backbone. Decoy-aware mapping was done in selective-alignment mode with '--mimicBT2', '--disableChainingHeuristic', and '--recoverOrphans' flags as well as sequence and position bias correction. For --fldMean and --fldSD, a value of 325 and 25 was used, respectively. Salmon's quants files were subsequently loaded into R (v 4.0.5) (R Core Team 2020) using the tximport package (v 1.18.0) (Soneson *et al*. 2015). Normalization of the reads was done with DeSeq2 (v 1.30.0) (Love *et al*. 2014) and foldchange-shrinkages were calculated with DeSeq2 and the apeglm package (v 1.12.0) (Zhu *et al*. 2019).

Acknowledgements

This work was funded by the Deutsche Forschungsgemeinschaft. The authors thank Mechthild Bömeke and Melanie Heinemann for technical support.

Data availability

Transcriptome data have been deposited in the National Center for Biotechnology Information's (NCBI) Sequence Read Archive (SRA) under accession no. SRR18189544 – SRR18189549. All other data of this study are available from the corresponding author upon reasonable request.

References

Arendsen, A.F., Soliman, M.Q., and Ragsdale, S.W. (1999) Nitrate-dependent regulation of acetate biosynthesis and nitrate respiration by *Clostridium thermoaceticum*. *J Bacteriol* **181**: 1489–1495.

Beaty, P.S., and Ljungdahl, L.G. (1991) Growth of *clostridium thermoaceticum* on methanol, ethanol or dimethylsulfoxide. *Ann Meet Am Soc Microbiol* **K-131**: 236.

Bertsch, J., and Müller, V. (2015) Bioenergetic constraints for conversion of syngas to biofuels in acetogenic bacteria. *Biotechnol Biofuels* **8**: 210.

Biegel, E., and Müller, V. (2010) Bacterial Na^+-translocating ferredoxin:NAD^+ oxidoreductase. *Proc Natl Acad Sci U S A* **107**: 18138–18142.

Biegel, E., Schmidt, S., González, J.M., and Müller, V. (2011) Biochemistry, evolution and physiological

function of the Rnf complex, a novel ion-motive electron transport complex in prokaryotes. *Cell Mol Life Sci* **68**: 613–634.

Bilous, P.T., Cole, S.T., Anderson, W.F., and Weiner, J.H. (1988) Nucleotide sequence of the *dmsABC* operon encoding the anaerobic dimethylsulphoxide reductase of *Escherichia coli*. *Mol Microbiol* **2**: 785–795.

Bilous, P.T., and Weiner, J.H. (1985a) Proton translocation coupled to dimethyl sulfoxide reduction in anaerobically grown *Escherichia coli* HB101. *J Bacteriol* **163**: 369–375.

Bilous, P.T., and Weiner, J.H. (1985b) Dimethyl sulfoxide reductase activity by anaerobically grown *Escherichia coli* HB101. *J Bacteriol* **162**: 1151–1155.

Bolger, A.M., Lohse, M., and Usadel, B. (2014) Trimmomatic: a flexible trimmer for Illumina sequence data. *Bioinformatics* **30**: 2114–2120.

Bradford, M.M. (1976) A rapid and sensitive method for the quantification of microgram quantities of protein utilizing the principle of proteine-dye-binding. *Anal Biochem* **72**: 248–254.

Bryant, M.P. (1972) Commentary on the Hungate technique for culture of anaerobic bacteria. *Am J Clin Nutr* **25**: 1324–1328.

Cammack, R., and Weiner, J.H. (1990) Electron paramagnetic resonance spectroscopic characterization of dimethyl sulfoxide reductase of *Escherichia coli*. *Biochemistry* **29**: 8410–8416.

Curson, A.R., Todd, J.D., Sullivan, M.J., and Johnston, A.W. (2011) Catabolism of dimethylsulphoniopropionate: microorganisms, enzymes and genes. *Nat Rev Microbiol* **9**: 849–859.

Daniel, S.L., Keith, E.S., Yang, H.C., Lin, Y.S., and Drake, H.L. (1991) Utilization of methoxylated aromatic compounds by the acetogen *clostridium thermoaceticum* - expression and specificity of the CO-dependent *O*-demethylating activity. *Biochem Biophys Res Commun* **180**: 416–422.

Das, A., and Ljungdahl, L.G. (1997) Composition and primary structure of the F_1F_0 ATP synthase from the obligately anaerobic bacterium *clostridium thermoaceticum*. *J Bacteriol* **179**: 3746–3755.

Dilling, S., Imkamp, F., Schmidt, S., and Müller, V. (2007) Regulation of caffeate respiration in the acetogenic bacterium *Acetobacterium woodii*. *Appl Environ Microbiol* **73**: 3630–3636.

Dorn, M., Andreesen, J.R., and Gottschalk, G. (1978) Fumarate reductase of *clostridium formicoaceticum*. A peripheral membrane protein. *Arch Microbiol* **119**: 7–11.

Drake, H.L., and Daniel, S.L. (2004) Physiology of the thermophilic acetogen *Moorella thermoacetica*. *Res Microbiol* **155**: 869–883.

Drake, H.L., Gößner, A.S., and Daniel, S.L. (2008) Old acetogens, new light. *Ann N Y Acad Sci* **1125**: 100–128.

Fontaine, F.E., Peterson, W.H., McCoy, E., Johnson, M.J., and Ritter, G.J. (1942) A new type of glucose fermentation by *clostridium thermoaceticum*. *J Bacteriol* **43**: 701–715.

Fröstl, J.M., Seifritz, C., and Drake, H.L. (1996) Effect of nitrate on the autotrophic metabolism of the acetogens *clostridium thermoautotrophicum* and *clostridium thermoaceticum*. *J Bacteriol* **178**: 4597–4603.

Fujita, D., Tobe, R., Tajima, H., Anma, Y., Nishida, R., and Mihara, H. (2021) Genetic analysis of tellurate reduction reveals the selenate/tellurate reductase genes *ynfEF* and the transcriptional regulation of *moeA* by NsrR in *Escherichia coli*. *J Biochem* **169**: 477–484.

Göbbels, L., Poehlein, A., Dumnitch, A., Egelkamp, R., Kröger, C., Haerdter, J., *et al*. (2021) Cysteine: an overlooked energy and carbon source. *Sci Rep* **11**: 2139.

Grimaldi, S., Schoepp-Cothenet, B., Ceccaldi, P., Guigliarelli, B., and Magalon, A. (2013) The prokaryotic Mo/W-bisPGD enzymes family: a catalytic workhorse in bioenergetic. *Biochim Biophys Acta* **1827**: 1048–1085.

Guymer, D., Maillard, J., and Sargent, F. (2009) A genetic analysis of in vivo selenate reduction by *salmonella enterica* serovar Typhimurium LT2 and *Escherichia coli* K12. *Arch Microbiol* **191**: 519–528.

Heise, R., Müller, V., and Gottschalk, G. (1992) Presence of a sodium-translocating ATPase in membrane vesicles of the homoacetogenic bacterium *Acetobacterium woodii*. *Eur J Biochem* **206**: 553–557.

Hess, V., Gonzalez, J.M., Parthasarathy, A., Buckel, W., and Müller, V. (2013) Caffeate respiration in the acetogenic bacterium *Acetobacterium woodii*: a coenzyme a loop saves energy for caffeate activation. *Appl Environ Microbiol* **79**: 1942–1947.

Hungate, R.E. (1969) A roll tube method for cultivation of strict anaerobes. In *Methods in Microbiology*, Norris, J.R., and Ribbons, D.W. (eds). New York and London: Academic Press, pp. 117–132.

Imkamp, F., Biegel, E., Jayamani, E., Buckel, W., and Müller, V. (2007) Dissection of the caffeate respiratory chain in the acetogen *Acetobacterium woodii*: indications for a Rnf-type NADH dehydrogenase as coupling site. *J Bacteriol* **189**: 8145–8153.

Imkamp, F., and Müller, V. (2002) Chemiosmotic energy conservation with Na^+ as the coupling ion during hydrogen-dependent caffeate reduction by *Acetobacterium woodii*. *J Bacteriol* **184**: 1947–1951.

Jonkers, H.M., van der Maarel, M.J.E.C., van Gemerden, H., and Hansen, T.A. (1996) Dimethylsulfoxide reduction by marine sulfate-reducing bacteria. *FEMS Microbiol Lett* **136**: 283–287.

Kappler, U., and Schäfer, H. (2014) Transformations of dimethylsulfide. *Met Ions Life Sci* **14**: 279–313.

Katsyv, A., and Müller, V. (2020) Overcoming energetic barriers in acetogenic C1 conversion. *Front Bioeng Biotechnol* **8**: 621166.

Ljungdahl, L.G. (1986) The autotrophic pathway of acetate synthesis in acetogenic bacteria. *Ann Rev Microbiol* **40**: 415–450.

Lorenzen, J., Steinwachs, S., and Unden, G. (1994) DMSO respiration by the anaerobic rumen bacterium *Wolinella succinogenes*. *Arch Microbiol* **162**: 277–281.

Love, M.I., Huber, W., and Anders, S. (2014) Moderated estimation of fold change and dispersion for RNA-seq data with DESeq2. *Genome Biol* **15**: 550.

Lubitz, S.P., and Weiner, J.H. (2003) The *Escherichia coli ynfEFGHI* operon encodes polypeptides which are paralogues of dimethyl sulfoxide reductase (DmsABC). *Arch Biochem Biophys* **418**: 205–216.

Magalon, A., Fedor, J.G., Walburger, A., and Weiner, J.A. (2011) Molybdenum enzymes in bacteria and their maturation. *Coord Chem Rev* **255**: 1159–1178.

McCrindle, S.L., Kappler, U., and McEwan, A.G. (2005) Microbial dimethylsulfoxide and trimethylamine-N-oxide respiration. *Adv Microb Physiol* **50**: 147–198.

Misoph, M., Daniel, S.L., and Drake, H.L. (1996) Bidirectional usage of ferulate by the acetogen *Peptostreptococcus productus* U-1: CO_2 and aromatic acrylate groups as competing electron accepters. *Microbiology* **142**: 1983–1988.

Müller, V. (2003) Energy conservation in acetogenic bacteria. *Appl Environ Microbiol* **69**: 6345–6353.

Patro, R., Duggal, G., Love, M.I., Irizarry, R.A., and Kingsford, C. (2017) Salmon provides fast and bias-aware quantification of transcript expression. *Nat Methods* **14**: 417–419.

Pierce, E., Xie, G., Barabote, R.D., Saunders, E., Han, C.S., Detter, J.C., *et al*. (2008) The complete genome sequence of *Moorella thermoacetica* (f. *clostridium thermoaceticum*). *Environ Microbiol* **10**: 2550–2573.

Poehlein, A., Bengelsdorf, F.R., Esser, C., Schiel-Bengelsdorf, B., Daniel, R., and Dürre, P. (2015) Complete genome sequence of the type strain of the acetogenic bacterium *Moorella thermoacetica* DSM 521T. *Genome Announc* **3**: e01159–e01115.

Puehringer, S., Metlitzky, M., and Schwarzenbacher, R. (2008) The pyrroloquinoline quinone biosynthesis pathway revisited: a structural approach. *BMC Biochem* **9**: 8.

R Core Team. (2020) *R: A Language and Environment for Statistical Computing*. Vienna, Austria: R Foundation for Statistical Computing. https://www.r-project.org.

Ragsdale, S.W., and Pierce, E. (2008) Acetogenesis and the Wood-Ljungdahl pathway of CO_2 fixation. *Biochim Biophys Acta* **1784**: 1873–1898.

Rosenbaum, F.P., and Müller, V. (2021) Energy conservation under extreme energy limitation: the role of cytochromes and quinones in acetogenic bacteria. *Extremophiles* **25**: 413–424.

Rosenbaum, F.P., Poehlein, A., Egelkamp, R., Daniel, R., Harder, S., Schluter, H., and Schoelmerich, M.C. (2021) Lactate metabolism in strictly anaerobic microorganisms with a soluble NAD($^+$) -dependent l-lactate dehydrogenase. *Environ Microbiol* **23**: 4661–4672.

Sakimoto, K.K., Wong, A.B., and Yang, P. (2016) Self-photosensitization of nonphotosynthetic bacteria for solar-to-chemical production. *Science* **351**: 74–77.

Sambasivarao, D., and Weiner, J.H. (1991) Dimethyl sulfoxide reductase of *Escherichia coli*: an investigation of function and assembly by use of in *vivo* complementation. *J Bacteriol* **173**: 5935–5943.

Schindelin, H., Kisker, C., Hilton, J., Rajagopalan, K.V., and Rees, D.C. (1996) Crystal structure of DMSO reductase: redox-linked changes in molybdopterin coordination. *Science* **272**: 1615–1621.

Schmidt, K., Liaaen-Jensen, S., and Schlegel, H.G. (1963) Die Carotinoide der *Thiorhodaceae*. *Arch Mikrobiol* **46**: 117–126.

Schoelmerich, M.C., and Müller, V. (2019) Energy conservation by a hydrogenase-dependent chemiosmotic mechanism in an ancient metabolic pathway. *Proc Natl Acad Sci U S A* **116**: 6329–6334.

Schuchmann, K., and Müller, V. (2014) Autotrophy at the thermodynamic limit of life: a model for energy conservation in acetogenic bacteria. *Nat Rev Microbiol* **12**: 809–821.

Schuchmann, K., and Müller, V. (2016) Energetics and application of heterotrophy in acetogenic bacteria. *Appl Environ Microbiol* **82**: 4056–4069.

Schwarz, F.M., Ciurus, S., Jain, S., Baum, C., Wiechmann, A., Basen, M., and Müller, V. (2020) Revealing formate production from carbon monoxide in wild type and mutants of Rnf- and Ech-containing acetogens, *Acetobacterium woodii* and *Thermoanaerobacter kivui*. *J Microbial Biotechnol* **13**: 2044–2056.

Seifritz, C., Daniel, S.L., Gößner, A., and Drake, H.L. (1993) Nitrate as a preferred electron sink for the acetogen *clostridium thermoaceticum*. *J Bacteriol* **175**: 8008–8013.

Simala-Grant, J.L., and Weiner, J.H. (1996) Kinetic analysis and substrate specificity of *Escherichia coli* dimethyl sulfoxide reductase. *Microbiology* **142**: 3231–3239.

Soneson, C., Love, M.I., and Robinson, M.D. (2015) Differential analyses for RNA-seq: transcript-level estimates improve gene-level inferences. *F1000Res* **4**: 1521.

Thauer, R.K., Kaster, A.K., Seedorf, H., Buckel, W., and Hedderich, R. (2008) Methanogenic archaea: ecologically relevant differences in energy conservation. *Nat Rev Microbiol* **6**: 579–591.

Tschech, A., and Pfennig, N. (1984) Growth yield increase linked to caffeate reduction in *Acetobacterium woodii*. *Arch Microbiol* **137**: 163–167.

Watts, S.F. (2000) The mass budgets of carbonyl sulfide, dimethyl sulfide, carbon disulfide and hydrogen sulfide. *Atmos Environ* **34**: 761–779.

Weiner, J.H., MacIsaac, D.P., Bishop, R.E., and Bilous, P.T. (1988) Purification and properties of *Escherichia coli* dimethyl sulfoxide reductase, an iron-sulfur molybdoenzyme with broad substrate specificity. *J Bacteriol* **170**: 1505–1510.

Weiner, J.H., Shaw, G., Turner, R.J., and Trieber, C.A. (1993) The topology of the anchor subunit of dimethyl sulfoxide reductase of *Escherichia coli*. *J Biol Chem* **268**: 3238–3244.

Wood, H.G., Ragsdale, S.W., and Pezacka, E. (1986) The acetyl-CoA pathway of autotrophic growth. *FEMS Microbiol Rev* **39**: 345–362.

Xiong, L., Jian, H., Zhang, Y., and Xiao, X. (2016) The two sets of DMSO respiratory systems of *Shewanella piezotolerans* WP3 are involved in deep sea environmental adaptation. *Front Microbiol* **7**: 1418.

Zhang, Y., Rump, S., and Gladyshev, V.N. (2011) Comparative genomics and evolution of molybdenum utilization. *Coord Chem Rev* **255**: 1206–1217.

Zhu, A., Ibrahim, J.G., and Love, M.I. (2019) Heavy-tailed prior distributions for sequence count data: removing the

noise and preserving large differences. *Bioinformatics* **35**: 2084–2092.

Zinder, S.H., and Brock, T.D. (1978) Dimethyl sulfoxide as an electron acceptor for anaerobic growth. *Arch Microbiol* **116**: 35–40.

Supporting Information

Additional Supporting Information may be found in the online version of this article at the publisher's web-site:

Supplementary Table S1